

# Thermally driven mesoscale flows — simulations and measurements

Karin Törnblom, Hans Bergström and Cecilia Johansson

*Department of Earth Sciences, Uppsala University, Villavägen 16, SE-752 36 Uppsala, Sweden*

*Received 24 Aug. 2006, accepted 2 May 2007 (Editor in charge of this article: Veli-Matti Kerminen)*

Törnblom, K., Bergström, H. & Johansson, C. 2007: Thermally driven mesoscale flows — simulations and measurements. *Boreal Env. Res.* 12: 623–641.

The wind climate shows often large local variations in coastal areas. The present study was based on measurements at several sites on the island of Gotland in the Baltic Sea and on simulations with a numerical meso- $\gamma$ -scale atmosphere model (the MIUU model). It is common for thermally driven flows, e.g. sea breezes and low level jets, to evolve resulting in supergeostrophic winds. The most important parameters affecting these flows were found to be temperature and roughness differences between the land and sea. Although the wind speed increases climatologically over a sea, a case where the wind speed decreased when advected out over a cold sea was investigated. This happens if the stable boundary layer (SBL) over the sea is deep enough. A deep SBL is favoured by strong thermal winds in combination with large temperature differences between the land and sea. With a shallow SBL the wind speed increases over the sea.

## Introduction

Sharp changes in temperature and surface roughness between land and sea make coastal areas suitable for studies of winds originating from thermally driven flows. These flows have a large influence on the local wind climate, which can differ from the synoptic winds seen in weather maps. Winds originating from thermally driven flows may often become supergeostrophic, i.e. stronger than the geostrophic wind driven by large-scale pressure gradients, and are interesting in several aspects, e.g. transport of pollutants, recreation, sound propagation and wind energy applications.

In high latitudes, large water bodies surrounded by land masses are likely to develop a particular meteorological regime during spring and large parts of the summer, when warm air is

advected out over the relatively much colder surface of the water. Thus stable stratification, with correspondingly low turbulent exchange rates at the surface, is bound to occur. The above situation has been found to apply to the Baltic Sea, which is a semi-enclosed sea located in northern Europe between roughly 55°N and 65°N.

Stable internal boundary layers (SIBL) over a cold sea were first studied by Csanady (1974) over Lake Ontario in Canada. Gryning and Joffre (1987) and Melas (1989) both studied the stable internal boundary layer over the Öresund Strait between Sweden and Denmark. A decrease of the wind speed over the sea was observed in the Öresund Experiment and is described in e.g. Doran and Gryning (1987) as well as in Gryning *et al.* (1987). Garratt (1987) and Garratt and Ryan (1989) applied a numerical model to aircraft data off the Australian coast. Garratt

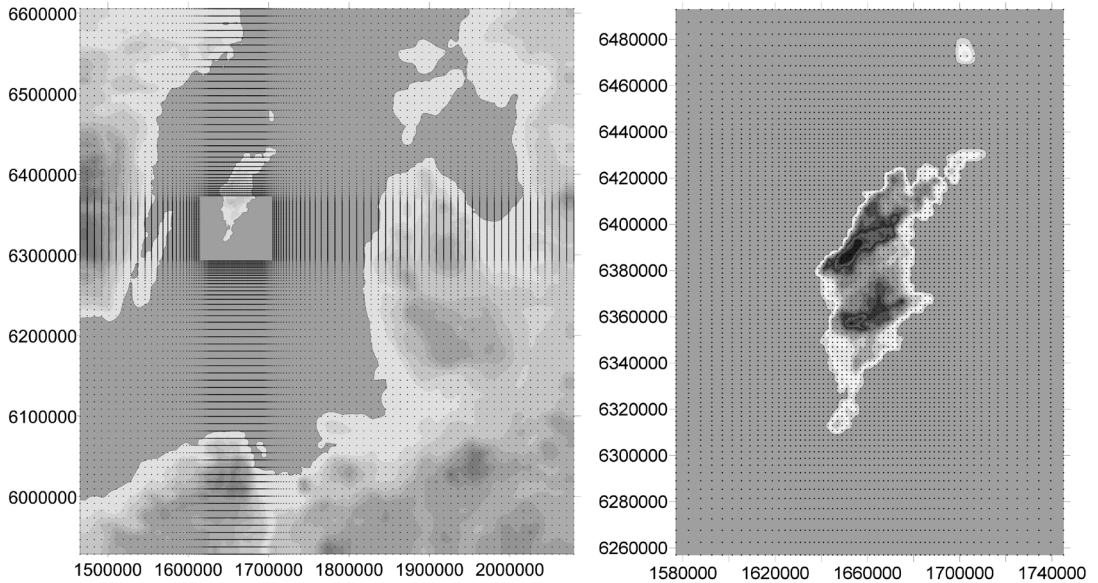


**Fig. 1.** Map over the Baltic Sea area and the island Gotland showing the model domains and the model grid points for the two model setups used. Distances are given in the Swedish geographical coordinate system (RT90) in metres. In the middle of the left side model domain (the square) the distance between the grid points is 1 km. In the square the grid points have been deleted in favour of seeing the contour of Gotland. Longitude and latitude for the centre of the square is 18°23' E and 57°14' N, respectively.

(1990) showed that the internal boundary layer height could be characterized by a critical layer flux Richardson number and distance from the shoreline. From his calculations the SIBL should grow fairly slowly with distance. Smedman *et al.* (1997) also investigated the evolution of a stable internal boundary layer over a cold sea with flow coming from a heated land area.

The present study is based on measurements at several sites on the island of Gotland in the Baltic Sea (Fig. 1) and on simulations with a numerical meso- $\gamma$ -scale atmosphere model. The purpose of the analysis is to highlight the complicated wind field over the Baltic Sea and the island of Gotland during a typical early summer situation with stable stratification over the sea and convection over land. Also the modification of the wind field due to various parameters is investigated. Investigated parameters are temperature differences between land and sea, roughness and topography differences, magnitude and direction of the geostrophic wind, and thermal wind.

Thermally driven flows and sea breezes have been studied in detail by many researchers over the years. About forty years ago Estoque (1962)

simulated sea breeze evolution assuming a background wind of  $5 \text{ m s}^{-1}$  from four directions parallel and perpendicular to the coastline. He found that an offshore wind favoured the evolution of a sea breeze. Arritt (1993) simulated thoroughly the evolution of a sea breeze with a 2D-mesoscale numerical model using background winds ranging from  $-15$  to  $+15 \text{ m s}^{-1}$ . A few studies have included effects from the shape of the coastline. Arritt (1989) found that curvature of the coastline produces slightly stronger winds offshore for a concave coast than for a convex coast. Savijärvi (2004) discussed surface winds across non-curved coastlines. Gillian *et al.* (2003) made a study of thermal circulations around the North Carolina coast, while Savijärvi *et al.* (2005) did a similar work for the Gulf of Finland.

Common in coastal areas during stable stratification are low-level jets (LLJ), i.e. wind maxima at lower altitudes, commonly 50–300 m above the surface. The classification of LLJs is not unambiguous, and different investigators have used different criteria. Some of them require the wind speed to be supergeostrophic, while for others it is enough that the wind speed

is  $2 \text{ m s}^{-1}$  higher at the maximum than above within the lowest 1500 m of the atmosphere (Stull 1988). Low-level jets can be caused by several phenomena. Over the coastal zone the most important ones are inertial oscillations, land and sea breezes, advective accelerations, coastal convergence, synoptic-scale baroclinicity and fronts. In this study LLJs are mostly developed in connection with sea breeze circulations.

The wind field over the Baltic Sea was studied extensively by Tjernström and Grisogono (1996) and Källstrand *et al.* (2000). The latter compared air-borne measurements and numerical simulations with an earlier version of the MIUU model (*see below*). They found a substantial decrease of the wind speed in the stably stratified marine boundary layer between the Swedish mainland and the island of Gotland, whereas the wind speed increased over Gotland. The conditions found by Källstrand *et al.* (2000) will be discussed further later in this paper.

## MIUU model

The MIUU model is a three-dimensional hydrostatic mesoscale model (Enger 1986). The model has prognostic equations for wind, temperature, humidity and turbulent kinetic energy. The turbulence is parameterised with a level 2.5 scheme according to Mellor and Yamada (1974), which implies that the turbulent kinetic energy is calculated by a prognostic equation, whereas other second order moments are obtained by diagnostic expressions described in detail by Andréon (1990). The MIUU model has a terrain-influenced coordinate system following the terrain at the surface but being horizontal at the model top (Pielke 1984). Of the 29 vertical levels used in the simulations, the lowest grid point is at the height  $z_0$ , where  $z_0$  is the roughness length, and the model top is at 10 000 m. A logarithmic spacing is used near the surface, with the second and third levels at 2- and 6-m heights, in order to accurately describe the physics at lower levels. For the upper vertical levels the spacing becomes linear.

The topography and land-use parameters were taken from digitised maps (the U.S. Geological Survey, the University of Nebraska-

Lincoln, and the European Commission's Joint Research Centre 1-km resolution global land cover characteristics database, 1999, available at <http://edcdaac.usgs.gov/glcc/glcc.html>). The land surface temperature and its daily variation were estimated with a surface energy balance routine that uses solar radiation and land use as input (Deardorff 1978). Over sea the observed average sea-surface temperatures were used. The model was initiated using temperature and humidity profiles representative for the modelled weather situations. Note that these profiles were only used for initialisation purposes. The model output was not used until 6 hours had passed (using a time step of 6 s), when the modelled conditions had adapted to the given surface boundary conditions. The large-scale synoptic pressure field was included as a geostrophic wind profile. The model was run for idealized, horizontally homogeneous synoptic conditions, but it could also have been run nested, e.g. using large-scale weather data as input. Therefore, in the simulations using a thermal wind discussed below, there was no complete matching to the large-scale horizontal temperature distribution. This was, however, judged to be of minor importance to the results.

Two model domain setups were used. For simulations over the entire Baltic Sea, the model domain was  $613 \times 675 \text{ km}$  and contained  $158 \times 165$  grid points. In the horizontal direction, a telescopic grid was used in order to achieve a high resolution over the area of interest. The grid spacing was 1 km between the grid points close to the centre of the domain, which was over the island of Gotland at the latitude of  $57^\circ 14' \text{N}$  and longitude of  $18^\circ 23' \text{E}$ . (Fig. 1a). The grid spacing then gradually expanded toward the boundaries, until reaching the largest spacing of 9 km. For simulations including Gotland only (Fig. 1b), the domain was  $168 \times 236 \text{ km}$  containing  $61 \times 95$  grid points with a 2-km spacing in the centre of the domain.

## Measurement characteristics

During the period of 17–26 May 2000 a measurement campaign was performed on the island of Gotland in order to investigate winds in the

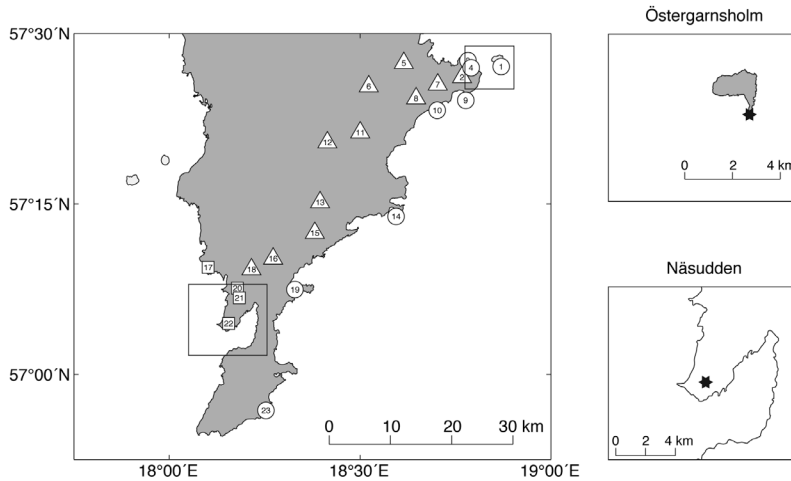


**Fig. 2.** Map over the southern part of Gotland showing sites where pibal trackings were taken. Squares are classified as west coast sites, triangles show inland sites, and circles indicate east coast sites. The stars in the two close-ups indicate the positions of towers with meteorological instrumentation.

area (Johansson and Bergström 2005). The most extensive measurements were made on 22 May. The synoptic situation was dominated by a weak high-pressure ridge over the Baltic Sea area, creating weak southwesterly winds over Gotland.

The measurements consisted of tower measurements and radio soundings at two sites, Näsudden and Östergarnsholm, and pibal tracking at several sites on the southern part of Gotland (Fig. 2). Östergarnsholm is a small island located about 4 km east of Gotland. It is a rather low island (5–10 m a.s.l.) and has no trees. A 30-m-high tower is erected on the southernmost tip of the island, giving an undisturbed over-water fetch for the wind direction sector 80–220°. The basic instrumentation consists of profile systems for wind speed, wind direction, temperature and turbulence.

The Näsudden tower is 145 m high and is located about 1.5 km from the shoreline on the Näsudden peninsula (Fig. 2). The surroundings are quite flat and partly covered with juniper bushes. There is an undisturbed open water fetch reaching the peninsula for winds coming from the sector 180°–330°. The instrumentation consists of profile systems for wind speed, wind direction and temperature. When the wind is coming from the sea, an internal boundary layer is built up over the land surface, reaching up to about 70 metres at the site of the tower. Above 70 metres the measurements are representative for marine conditions (Bergström *et al.* 1988).

The wind speed and direction were also

measured at around 20 sites on the southern part of Gotland (Fig. 2) using a single theodolite pibal tracking technique. (Alexandersson and Bergström 1979). In this techniques, balloons filled with hydrogen are released and followed with a theodolite as they ascend through the atmosphere and follow the winds at the same time. Balloons with a radius of 0.8 m and average ascent rate of 4 m s<sup>-1</sup> were used. The theodolite was manually directed towards the balloon and the azimuth angle, elevation angle and time were stored on a Campbell CR510 logger every 10 seconds. The final wind profile consisted usually of an average of two or three tracked balloons in order to reduce uncertainties, which typically were about  $\pm 0.5$  m s<sup>-1</sup> below the 1000 m height. A balloon ascent up to about 2500 m takes about 10 min, which means that the final wind profile was an average of approximately a 20–30 min.

## Results — Baltic domain

### Case 1: Increasing wind speed over sea

In order to compare model results with observations on 22 May, the MIUU model was run for a 30-hour period with input data chosen to represent the large-scale conditions of that day. The background flow was specified as the geostrophic wind with a speed 2.5 m s<sup>-1</sup> from the southwest, having no shear with the height, i.e. no thermal wind was applied. The model was

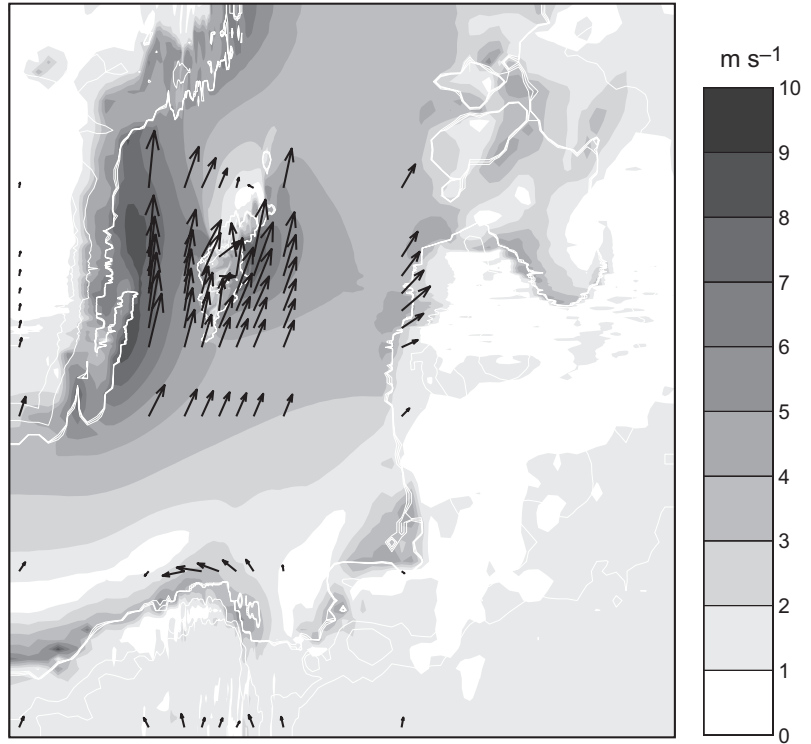


**Fig. 3.** Modelled wind field over the Baltic Sea area at 16:00 LST at the height of 72 m for a geostrophic wind speed of  $2.5 \text{ m s}^{-1}$  from southwest.

run with a prescribed and constant temperature of  $11 \text{ }^\circ\text{C}$  for the water surface, while the surface temperature over land areas was calculated from the energy balance routine. The cloudiness during the simulations was set to 50%. The model was initialised with a temperature profile having a lapse rate of about  $0.0025 \text{ K m}^{-1}$  up to about 2000 m height.

The modelled wind field at 72 metres at 16:00 LST (Local Standard Time = UTC + 1 hour) over the Baltic Sea area (Fig. 3) shows that the land/sea temperature differences induced a local pressure difference between the land and sea at low levels, with a low pressure over land. A sea breeze circulation started at the eastern coast of Gotland, but since the geostrophic wind was coming from the southwest, the resulting wind direction originating from the combined effect of the sea breeze and geostrophic wind was almost from the south and parallel to the coast. This is because the sea breeze, which was easterly to start with, turned clockwise during the day due to the Coriolis force, making it southeasterly in the afternoon. The resulting LLJ had its maximum strength at around 70 m, but

high winds almost reached the ground, (compare Fig. 4e and f).

The wind speed is generally much higher over the water compared with that over the land (Fig. 3). The thermally driven flow originating from the Swedish mainland influences the entire Baltic Sea. Besides the fairly strong thermally-driven low level jet developing on the east coast of Gotland, a weak sea breeze can be seen to the north of the island. At the coast of the Baltic States another sea breeze is created.

#### Comparison of model results with measurements

The time evolution of measured and simulated winds at three sites on Gotland is presented as time-height cross sections (Fig. 4). At Näsudden (Fig. 4a and b), the observed wind at lower levels was around  $3 \text{ m s}^{-1}$ . At the height of around 200 m, there were low winds during the day that increased during the late afternoon. This increase was also seen in the model result. At Sigter further inland from Näsudden (Fig. 4c and d),

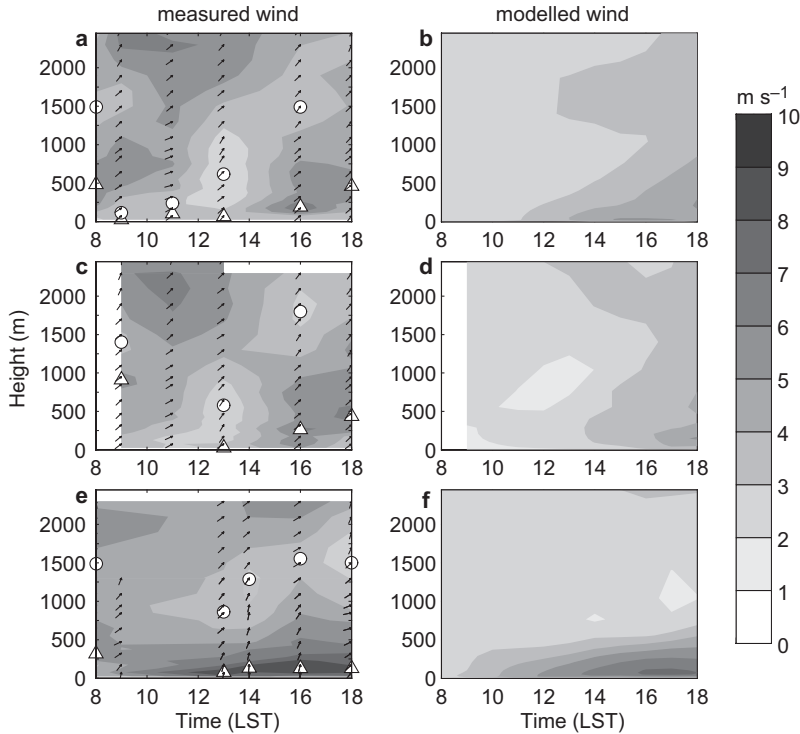


**Fig. 4.** Time-height cross sections showing the evolution of the wind at Näsudden (**a** and **b**), at Sigtun (**c** and **d**), and at Östergarnsholm (**e** and **f**) on 22 May 2000. Triangles indicate height of low-level wind maximum. Circles indicate height of wind speed minimum above the maximum. The arrows indicate the wind direction, where a downward-pointing arrow indicates northerly winds, while an arrow pointing left indicates easterly winds, etc.

there was not much of a change in the observed winds compared with Näsudden. But besides the increase in the wind during the afternoon, the model here also caught the minimum around the noon. On Östergarnsholm off the east coast (Fig. 4e and f), a jet due to a “sea breeze” was evolving during the day, creating rather strong winds at lower levels. This structure was very well caught by the model.

Worth noticing is that the model was run with a constant geostrophic forcing, which does not change neither in the horizontal nor in the vertical, and is also constant with time. Therefore some structures in the wind field at higher heights, as well as during the morning hours, were not found in the simulations. However, the resemblances between the measured and modelled winds were good below 1000 m and from the late morning during the rest of the day. More validations of the model with satisfactory result can be found elsewhere in the literature (e.g. Smedman *et al.* 1996, Enger *et al.* 1993, Koracin and Enger 1994, Bergström 1996, Sandström 1997, Källstrand *et al.* 2000.)

The difference between the west coast (Näsudden) and the east coast (Östergarnsholm)

will be discussed in more detail later, and could be explained by the development of a thermally-driven flow due to the presence of Gotland surrounded by the colder sea.

### Measured low level jets

From the 110 wind profiles measured using the pibal tracking, Johansson and Bergström (2005) found that 65% of the profiles contained a low level jet, i.e. a wind speed maximum below the 500 m height, created by mesoscale effects. Out of the 47 profiles from the east coast sites the same figure was 83%. The wind direction during this time was dominantly from the southwest.

The observed difference between the maximum wind speed in the LLJ and minimum wind speed above the jet was also analysed. It can be seen (Fig. 5) that the maximum in the wind speed increased during the day being largest at around 16:00 LST. The wind in the jet was, as the mean of all the east-coast profiles, up to  $5.5 \text{ m s}^{-1}$  higher at the maximum than at the minimum above. Although the jet was strongest at the east coast, it still existed at the inland sites.

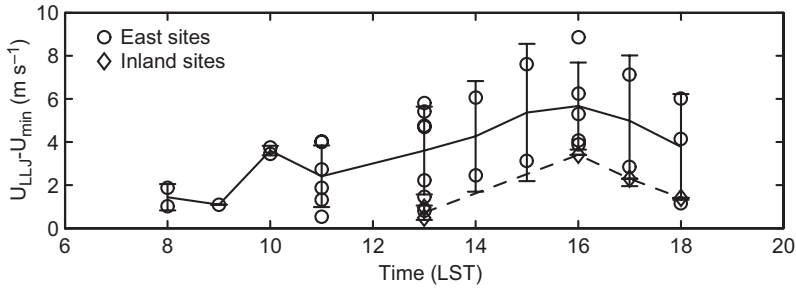


**Fig. 5.** Observed daily variation of the difference in wind speed between the maximum in the LLJ and the minimum above the jet for east coast sites and inland sites. The symbols indicate individual measurements and the lines give average values. The solid and the dashed lines show, respectively, the mean of all east coast sites and all the inland sites containing low level jets. The inland sites are typically located 5–10 km from the southeast coast of Gotland.

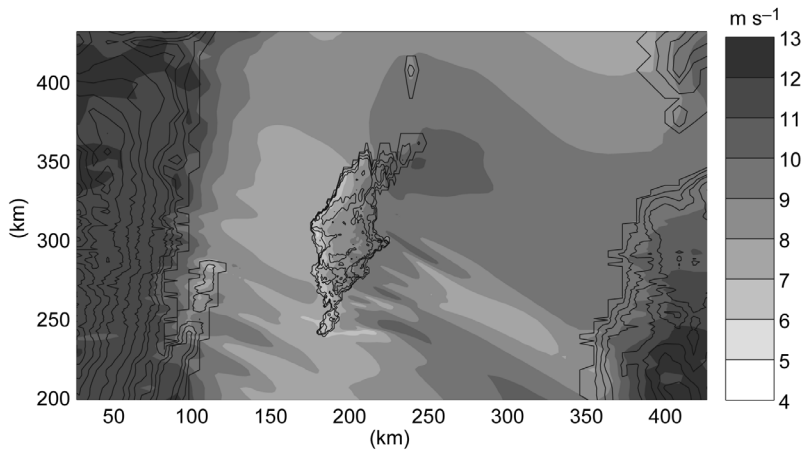


**Fig. 6.** Modelled wind field at the 49 m height for 3 May 1997 at 14:00 LST. Geostrophic wind from northwest.

## Case 2: Decreasing wind speed over sea

In the case study made above, the strongest winds were found over the sea while the wind speed was lower over the land. Although climatological results have shown clearly that winds are generally stronger over the sea than over the land (*see e.g. Bergström 2001*), this is not always the case. Källstrand *et al.* (2000) described an experiment with airborne measurements for 3 May 1997, a day with strong winds. They found that the wind speed decreased at low levels when advected out over sea, where a stable boundary layer (SBL) was evolving. Winds decreasing with the offshore distance can be explained by a reduced momentum transfer inside a stable boundary layer. This phenomenon was also caught in simulations with the MIUU model. In this case the geostrophic wind at surface level was  $15 \text{ m s}^{-1}$  and increased to  $46 \text{ m s}^{-1}$  at the 3000 m height. The sea sur-

face temperature was  $4 \text{ }^\circ\text{C}$ , whereas the land was heated to about  $10 \text{ }^\circ\text{C}$  during the day.

In order to investigate the reasons for the findings by Källstrand *et al.* (2000), a sensitivity study using the MIUU model was carried out. A 3D simulation with the Baltic domain was performed in order to recapture the scenario of 3 May 1997. The geostrophic wind was from northwest. It is clearly seen in the modelled wind field at the 49-m height at 14:00 LST how the wind speed decreased when the air advected out over sea from the coast of the Swedish mainland (Fig. 6). The wind speed over the mainland was about  $10 \text{ m s}^{-1}$ , decreasing to  $7 \text{ m s}^{-1}$  before entering the west coast of Gotland where the wind speed again increases over land.

A similar simulation was made without the thermal wind, i.e. the geostrophic wind was set to a constant value of  $15 \text{ m s}^{-1}$  at all heights in the model. The resulting wind field at the 49-m

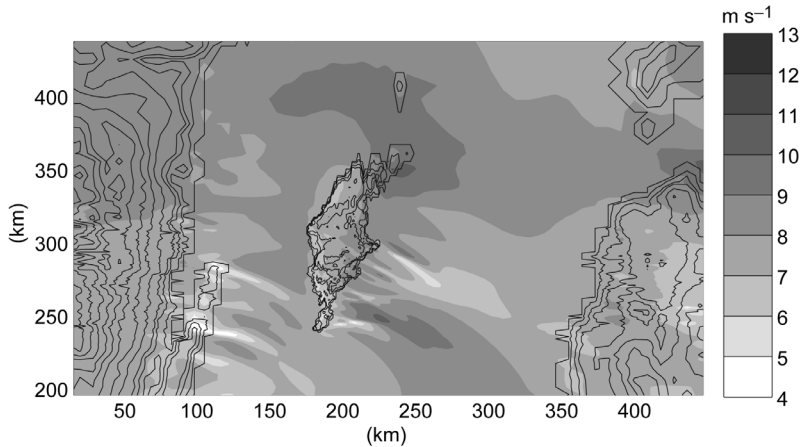


**Fig. 7.** Same as Fig. 6 but with no thermal wind.

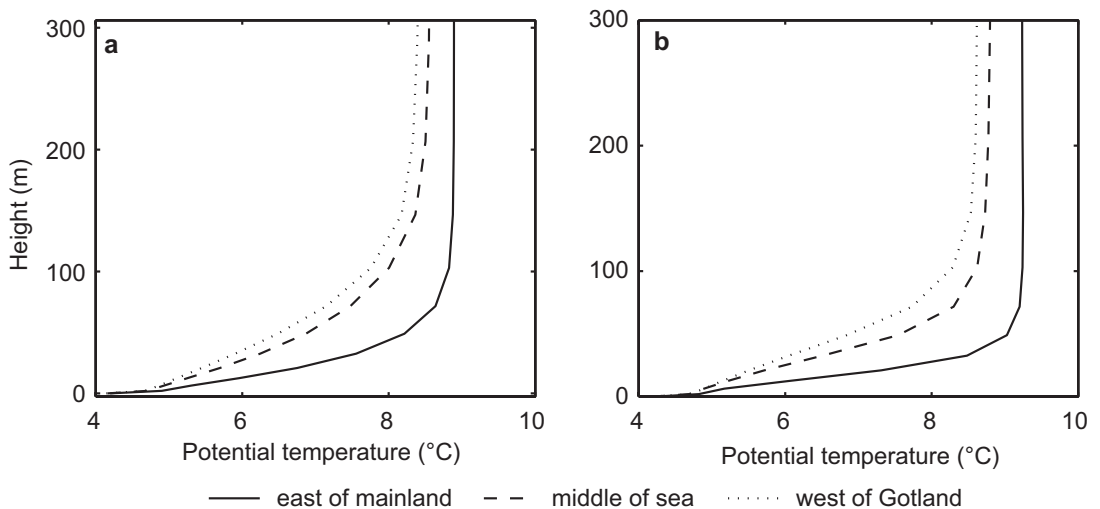


**Fig. 8.** The evolution of the SBL from the east coast of the Swedish mainland to the west coast of Gotland. — **a:** results from the simulation with thermal wind. — **b:** the results without thermal wind.

height at 14:00 LST is seen in Fig. 7. In this case the wind did not significantly slow down when coming out over the sea, nor did it increase again over Gotland.

The absence of a large-scale thermal wind means that less momentum may be transported downwards to lower levels in the atmosphere. Especially in the turbulent unstable boundary-layer over land, this results in a lower wind speed for the barotropic case (Fig. 7) as compared with the case with a thermal wind (Fig. 6). The land and sea temperatures were about the same in the two simulations.

The thermal wind also affects the height and growth of the SBL over sea. A thermal wind enhances mixing, resulting in a deeper and

somewhat colder stable layer (*see* Fig. 8). For the case with a thermal wind, the modelled SBL grew from around 100 m to around 200 m from east of the Swedish mainland to a point just west of Gotland. For the barotropic case the modelled SBL height was 75 and 150 m at the same locations.

In order to further investigate the influences of the thermal wind, and also other parameters such as the geostrophic wind speed, temperature differences between the land and sea as well as large-scale temperature profile, several 2D simulations were performed with the MIUU model.

Changing the gradient of the geostrophic wind (the thermal wind) between  $0.01 \text{ s}^{-1}$  to  $0 \text{ s}^{-1}$  in the simulations, we can see that the wind

decreased when advected out over sea in all cases, but the significance was much higher for the large vertical gradients of the geostrophic wind (Table 1). It can also be seen that the depth of the convective mixed layer over the Swedish mainland increased with an increasing thermal wind speed.

Simulations were also made with a constant thermal wind speed, i.e. the geostrophic wind speed increased by  $31 \text{ m s}^{-1}$  in the lowest 3000 m, but with different strengths of the geostrophic wind (Table 2). When the geostrophic wind was reduced in strength, but with the strong thermal wind remaining, the offshore decrease in wind speed was even more dominant. However, as the geostrophic wind decreases, sea breezes started to evolve near the coasts. This led, of course, to quite a different scenario.

The temperature difference between the land and sea may also be an important parameter. In the case described by Källstrand *et al.* (2000), the surface temperature over Gotland at 14:00 LST was around  $9^\circ\text{C}$  while the sea surface temperature was  $4^\circ\text{C}$ . Decreasing the land surface temperature resulted in a shallower SBL (not shown) and the wind speed did not decrease as much over the sea (Table 3). The same took

place if the temperature profile used as an initialization in the model was more stable.

As mentioned earlier, climatologically the wind speed obviously increases over the sea. The difference in the cases discussed here compared to the “normal” case was that a relatively deep internal SBL was building up over the sea. The depth of the SBL was enhanced by a strong thermal wind and large temperature difference between the land and sea. If the SBL is more shallow (as e.g. in the case shown in Fig. 3), the wind will increase over sea, except in a shallow layer close to the surface.

## Simulations with Gotland as an isolated island

Simulations with Gotland as an isolated island in a large sea were made in order to get a refined picture and understanding of the processes affecting the wind fields around an island and generally in coastal areas. The scenario was based on the simulation of 22 May when the mid-day elevation of the sun was large resulting in high insolation. At the same time the sea was still cold after the winter and the temperature

**Table 1.** The effect of thermal wind on offshore decrease of wind speed at the 49-m height.

| Thermal wind speed from surface to the height of 3000 m ( $\text{m s}^{-1}$ ) | Wind speed offshore east coast of the mainland ( $\text{m s}^{-1}$ ) | Wind speed offshore west coast of Gotland ( $\text{m s}^{-1}$ ) | Wind speed over Gotland ( $\text{m s}^{-1}$ ) | Surface temperature on Gotland ( $^\circ\text{C}$ ) | Depth of convective layer over the mainland (m) |
|---|--|---|---|---|---|
| 15 to 46  | 10.4   | 7.9   | 10.2  | 9   | 4000  |
| 15 to 25  | 8.1  | 7.2   | 8.2   | 9   | 2500  |
| 15 to 15  | 7.2  | 7.0   | 7.5   | 9   | 2000  |

**Table 2.** The effect of geostrophic wind on offshore decrease of wind speed.

| Thermal wind speed from surface to the height of 3000 m ( $\text{m s}^{-1}$ ) | Wind speed offshore east coast of the mainland ( $\text{m s}^{-1}$ ) | Wind speed offshore west coast of Gotland ( $\text{m s}^{-1}$ ) | Wind speed over Gotland ( $\text{m s}^{-1}$ ) | Surface temperature on Gotland ( $^\circ\text{C}$ ) | Depth of convective layer over the mainland (m) |
|---|--|---|---|---|---|
| 15 to 46  | 10.4   | 7.9   | 10.2  | 9   | 4000  |
| 10 to 41  | 6.0  | 2.4   | 6.7   | 9   | 3500  |
| 5 to 36   | 3.7  | 1.5   | 3.8   | 9   | 3800  |

differences between the land and sea were commonly large during the daytime. Tests were made with background winds coming from five different directions (west, southwest, south, southeast and east) and having different strengths (2.5–10 m s<sup>-1</sup>). The influence of surface properties was also studied by deleting parameters such as the surface roughness, topography and daytime heating of the island.

### Time evolution of the thermally driven flow

In order to show the time evolution of the thermally driven flow, a simulation with a 2.5 m s<sup>-1</sup> geostrophic wind from southwest was chosen. This is the case for which the largest thermally driven flow evolved and the physics was therefore well illustrated. This case was comparable with the weather situation on 22 May, except that it was simulated using a smaller computational domain.

In the morning, the sun started to heat Gotland. This led to the evolution of a convective layer that grew in height with time. In combination with the higher roughness of the island, the wind speed decreased over the land and the flow tended to go around the island instead (09:00 LST), creating two weak low-level jets at both sides of the island, leaving very weak winds over the land (Fig. 9).

As the land surface became warmer (12:00 LST), the convective layer increased further in depth, building up a thermal low over the island, and the temperature gradient between the land and sea increased. This in turn gave rise to a ther-

mally driven flow at the east coast of Gotland, enhanced by the background flow. The jet at the west coast weakened because it was opposed by the background flow. At this time the coastal winds had started to veer against the coast of the island, creating a front (convergence zone) with a low wind speed over the interior of the island where the sea breeze circulations met. This feature grew during the day when the land surface temperature reached a maximum of 15.5 °C and the convective boundary layer grew up to 1000 m (15:00 LST). Further to the north in the lee of the island, an area with low northerly winds was found. There a light sea breeze started and evolved during the day, affecting the flow also during the evening.

In the evening (20:00 LST) when the warming of the land ceased, the forcing of the thermally driven flow disappeared and the jet at the east coast weakened. Without the thermal forcing from the island, the remnant of the jet was advected away with the background flow (00:00 LST).

Note that the difference between the west coast and the east coast, seen in the measurements for southwesterly winds (Fig. 4), was caught by the model simulation. The resemblance between the simulation and the measurements in terms of how the east coast jet spread in over land in late afternoon is also worth noticing. It can be clearly seen from the dashed curve in Fig. 5 that the jet existed also over land and evolved in the same manner as over the sea, but with the difference that the jet over land was somewhat smaller in magnitude. In the simulation (Fig. 9) the jet also spread over land in the early evening. Also the turning of the wind towards the south

**Table 3.** The effect of temperature differences between land and sea on offshore decrease of wind speed.

| Thermal wind speed from surface to the height of 3000 m (m s <sup>-1</sup> ) | Wind speed offshore east coast of the mainland (m s <sup>-1</sup> ) | Wind speed offshore west coast of Gotland (m s <sup>-1</sup> ) | Wind speed over Gotland (m s <sup>-1</sup> ) | Surface temperature on Gotland (°C) | Depth of convective layer over the mainland (m) |
|--|---|--|--|-------------------------------------|---|
| 15 to 35   | 8.1   | 5.2  | 8.8  | 9–10                                | 3000  |
| 15 to 35   | 8.3   | 5.7  | 9.0  | 9                                   | 3000  |
| 15 to 35   | 8.7   | 6.6  | 9.1  | 8                                   | 2500  |
| 15 to 35   | 8.5   | 6.9  | 9.3  | 6–7                                 | 2300  |
| 15 to 35   | 8.5   | 7.8  | 9.7  | 5–6                                 | 1800  |

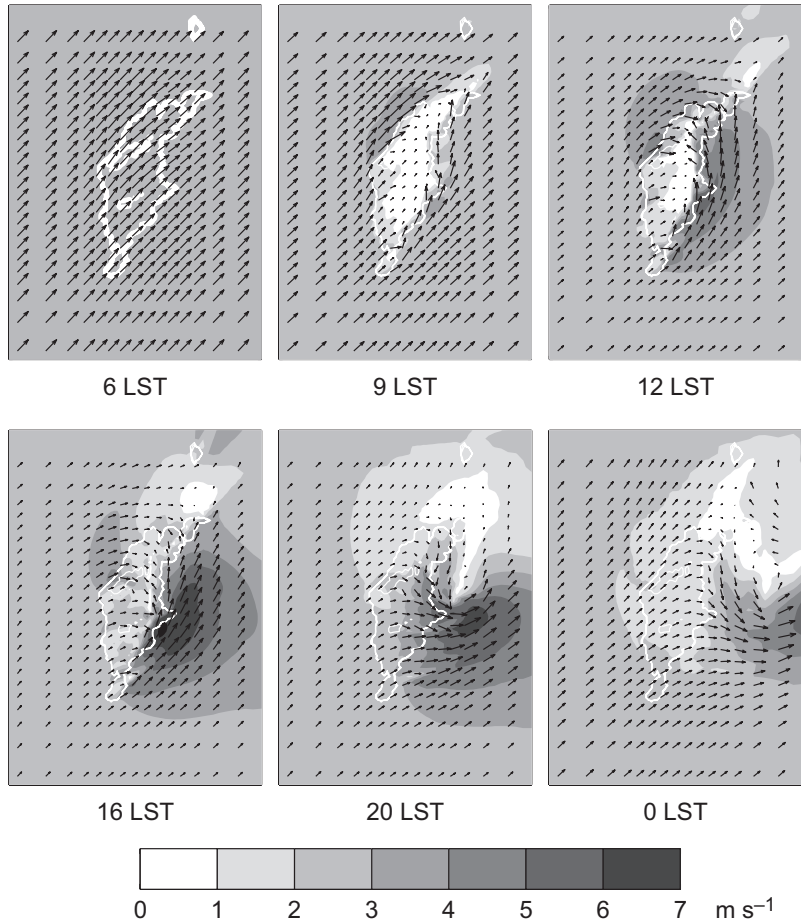


**Fig. 9.** Time evolution of the modelled wind field at the height of 72 metres. A geostrophic wind speed of  $2.5 \text{ m s}^{-1}$  from the southwest was assumed. The grey scale in the plots shows the wind speed, whereas the arrows indicate the wind direction.

at the east coast, as seen in model results (Fig. 9), was observed in the measurements (arrows in Fig. 4e).

### The effect of the background wind

In order to illustrate the influence of the background forcing, simulations with geostrophic winds of different strength and direction (westerly, southwesterly, southerly, southeasterly and easterly background winds) were made. The magnitudes of the forcing were set to  $2.5$ ,  $5$ ,  $7.5$  and  $10 \text{ m s}^{-1}$ . For the simulations with a geostrophic forcing of  $2.5$  and  $5 \text{ m s}^{-1}$ , large thermally driven flows were created. For stronger forcing, this feature was not as pronounced, a result that agrees well with earlier studies (e.g. Arritt 1993).

The wind field at a height of 72 metres over Gotland and the surrounding sea at 16:00 LST for the forcing of the geostrophic wind speed of  $2.5 \text{ m s}^{-1}$  coming from five different directions: west, southwest, south, southeast and east, was investigated (Fig. 10). The highest wind speeds were found at this time and height for all five simulations. The presence of the island induced thermally driven flows for all directions of the forcing, even though this feature was strongest for southwesterly background winds. Most probably this is due to the shape of the island and the coastline curvature.

In all five scenarios, a high-wind zone evolved when the wind came in contact with the right-hand side of the island and approached the lee side. Here the wind speed became super-geostrophic (i.e. higher than the background wind) in all the cases, with a low-level jet maxi-

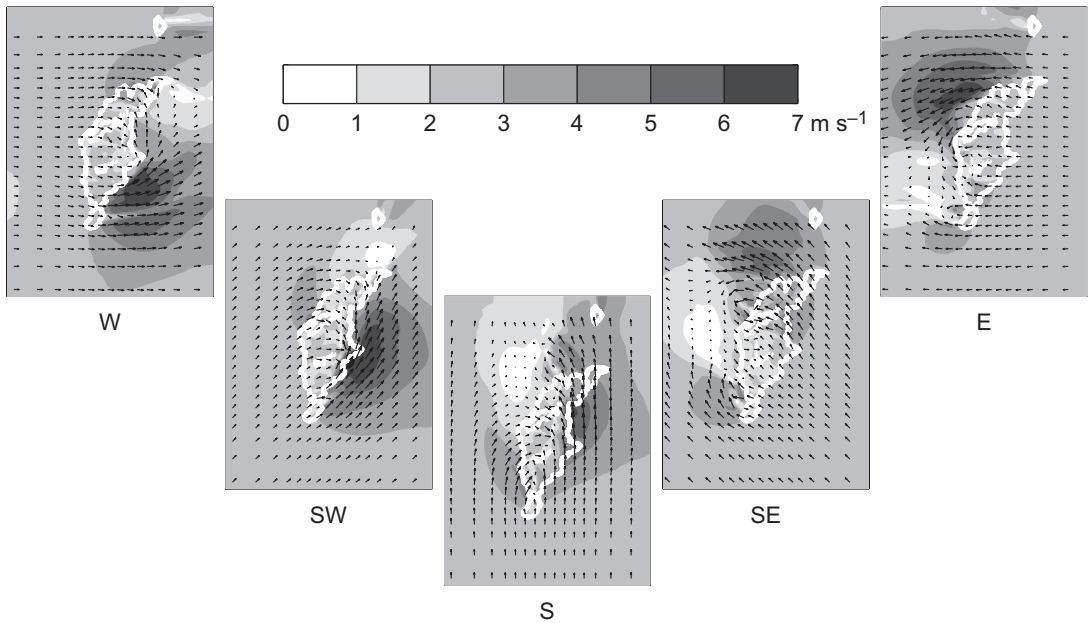


**Fig. 10.** Modelled wind at 16:00 at the height of 72 m for the geostrophic wind forcing of  $2.5 \text{ m s}^{-1}$  coming from west, southwest, south, southeast and east.

mum at a height of around 50–100 m and veering of the wind towards the coast of the island. Further downstream the jet, on the very lee side of the island, an area with low wind speeds was found for all directions of the background flow, and just as in the case described in the previous section, a weak sea-breeze circulation was started in this area.

The wind field in a vertical south–north cross section just east of Gotland at 16:00 LST for the geostrophic wind speed of  $2.5 \text{ m s}^{-1}$  from southwest, shows that above the low wind area, seen in Fig. 10, there was a second jet at around 1000 m height (Fig. 11). Also, there was a belt of low winds reaching all the way up to about 2000 m, quite high above the large thermally driven jet. This was due to the return flow associated with the sea breeze opposing here the large-scale southwesterly wind.

For the stronger forcing of  $7.5 \text{ m s}^{-1}$  from the southwest (Fig. 12), the effects of topography and surface roughness dominated over those of thermally driven flows. The wind speed decreased when approaching the windward coast, and over the interior of the island its strength at the 72-m height was approximately half of that over the sea. For continuity reasons the winds

were higher than the geostrophic forcing at both sides of the island. In the lee of the island, a band of low winds was found.

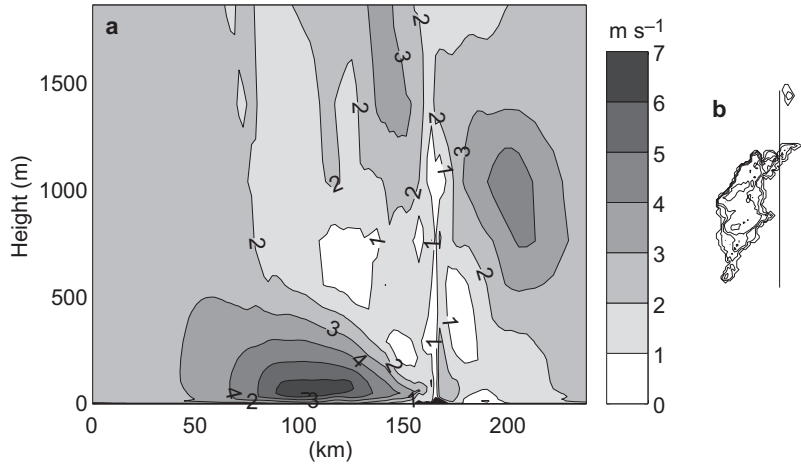
## Divergence

The effects of thermally induced flows may also be studied by looking at the horizontal divergence expressed as

$$\vec{\nabla} \cdot \vec{U} = \frac{\partial u}{\partial x} + \frac{\partial v}{\partial y}, \quad (1)$$

where  $\vec{U}$  is the total wind vector, and  $u$  and  $v$  are the components of the wind speed in the  $x$  and  $y$  direction, respectively. The horizontal divergence for the simulation of 22 May, with the geostrophic wind speed  $2.5 \text{ m s}^{-1}$  from southwest (see Fig. 9, 16:00), shows that at the windward coast a weak convergence zone was formed (Fig. 13a) when the offshore wind entered the coast and met the flow with lower wind speeds over the island, resulting from turbulence coming mostly from convection but also from an increase in surface roughness (light colour in the plot). At the leeward coast where the strongest winds evolved, there was a sharp

**Fig. 11.** A height cross-section along a south-north line at the eastern coast of Gotland (shown on the map to the right) showing the modelled wind speed at 16:00 LST for the geostrophic wind speed of  $2.5 \text{ m s}^{-1}$  from southwest.



edge between divergence and convergence. The wind near the coastline turned towards the coast and met with the wind coming over the island from the windward side, creating a convergence zone over the coastal strip (white in the plot). Over the sea where the LLJ was located, divergence was found (black in the plot).

Also, there were bands of convergence reaching from coast to coast, created by the thermally driven flows. The northernmost of these bands was found where the flow from the northern sea breeze met with the inland flow. The southernmost band might have been related to the topography. These bands of convergence coincided with the bands of low winds (see Fig. 9, 16:00 LST) and were probably also associated with convective cloud formation.

In the evening at 20:00 LST the pattern was somewhat different (Fig. 13b). There was convergence neither at the windward coast nor on the leeward coast. The convection had been ceased. The bands of convergence seen earlier in the day were displaced by the general flow, advected eastward as the stratification above the island started to stabilize. However, the convergence was still strong at the location where the northern sea breeze flow met with the flow from over the island.

Comparisons between our results and those presented by Samuelsson and Tjernström (2001) showed some resemblance. They performed a study of horizontal divergence over a Swedish lake in June and got a dipole pattern with divergence upstream the lake and convergence

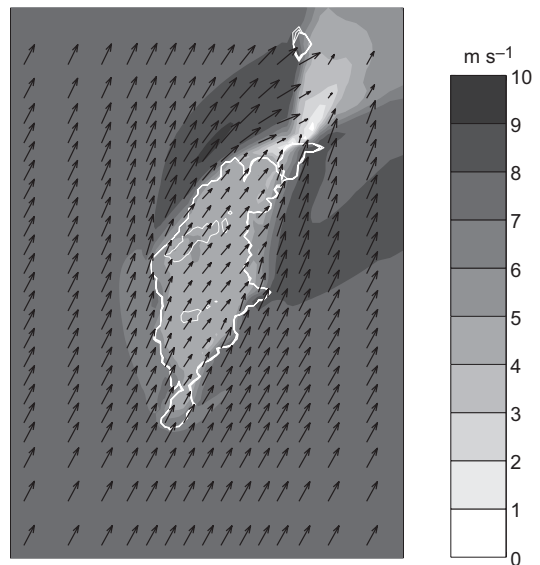


**Fig. 12.** The modelled wind field at the 72 m height at 16:00 LST. The geostrophic wind speed was  $7.5 \text{ m s}^{-1}$  from the southwest.

downstream. This pattern was most pronounced in early morning. They explained this by reduced roughness over the lake, and that convection helped the acceleration over the lake during the night time, while in daytime the stably-stratified air over the lake progressively impeded the acceleration.

In the present study the same features, with convergence at the upwind coast (when the wind comes from the sea, reaching the coast) and divergence at the downwind coast could be seen. However, the divergence field got more complex

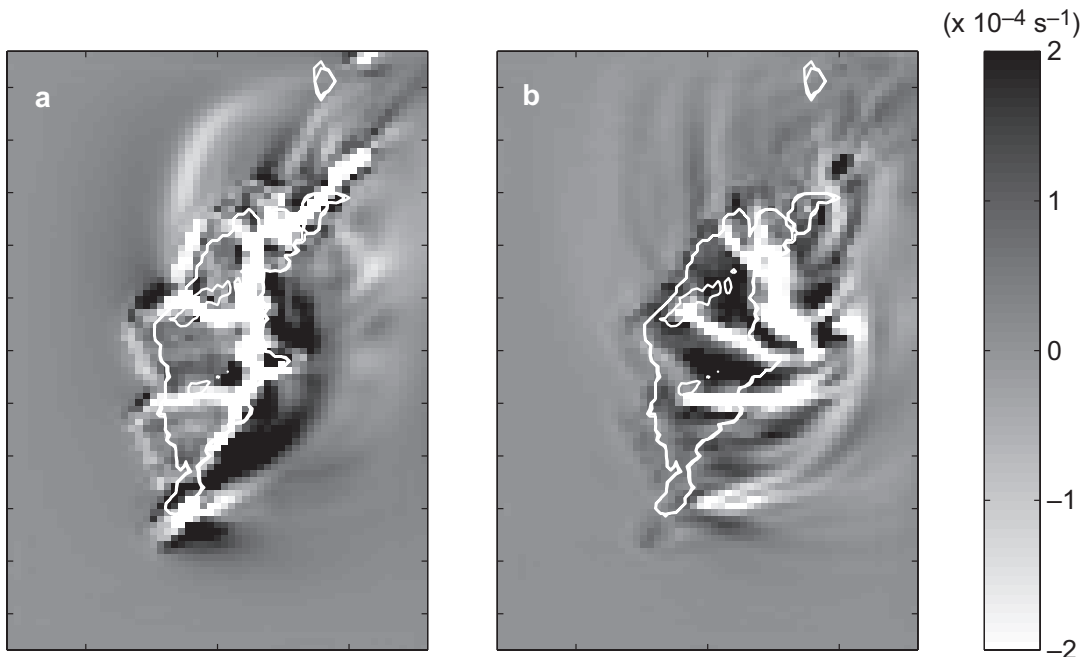


**Fig. 13.** Divergence ( $\text{s}^{-1}$ ) of the modelled wind field at the 72 m height at (a) 16:00 LST and (b) 20:00 LST. Model results are for a south-westerly geostrophic wind speed of  $2.5 \text{ m s}^{-1}$ .

than in the lake study. There are several reasons for this. In the present study, the island had a higher surface roughness and topography than the surrounding sea, which was just the opposite to the study of the lake. Furthermore, the coastlines were more complex and the island was larger, giving rise to larger thermally driven flows that changes the divergence field.

### Surface properties

In order to further illustrate the physics behind the modifications of the wind field due to the presence of an isolated island in the sea, the surface properties of the island were changed. The results were illustrated by the wind field at 16:00 LST at the height of 72 m above the island Gotland for a geostrophic forcing of  $5 \text{ m s}^{-1}$  from southwest and for different surface properties (Fig. 14).

If the diurnal heat changes were taken away from the island, i.e. setting the temperature to a constant value equal to the sea water temperature (Fig. 14b), but the topography and surface roughness were kept intact, the wind did not

slow down over the island in the same manner at this height as in the real case (Fig. 14a). However, there was still a small (very local in height) wind maximum just north west of the island.

By removing only the topography (Fig. 14c), the flow did not change significantly from the real case (Fig. 14a). Of course, this does not have to be a general result, since the topography is quite moderate on Gotland (as most about 50–70 m above the sea level).

When the surface roughness of the island was decreased to the same value as for water, but the heat was allowed to change diurnally (Fig. 14d), it was seen that the strength of the thermally driven flow was dependent also on factors other than the temperature difference between the land and sea. This is because the maximum was much smaller now than with the real island. The surface roughness played also an important role for the development of the wind field. An increased roughness resulted in a lower wind speed over the island up to a certain height, depending on the background wind. Parts of the air then took the path around the island instead of over it, producing a maximum at the eastern and western coast of Gotland.

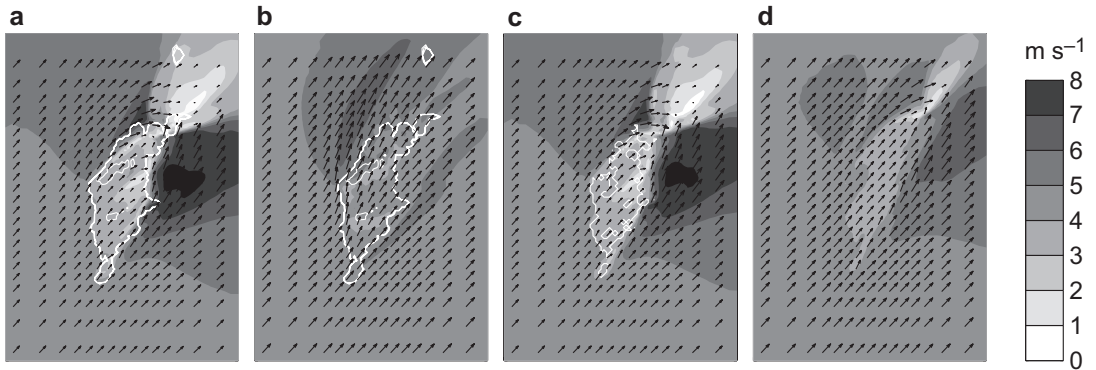


**Fig. 14.** Modelled wind speed at the 72 m height at 16:00 LST for a geostrophic wind forcing of  $5 \text{ m s}^{-1}$  and for different surface properties: (a) a real Gotland, (b) no heating, (c) no topography, (d) no topography and no surface roughness.

It can be concluded that the heating of the island, together with the surface roughness, played the most important roles in the modification of the wind fields in these simulations.

However, as discussed by Stein and Alpert (1993), it may be misleading to take away only one parameter at a time in order to see the influence on some other parameter, in this case the wind field. The parameters do, of course, interact. Therefore it is of great importance to test all possible combinations of the chosen parameters. The results of such tests (Table 4) indicate similar results as seen earlier when looking at the plots (Fig. 14). Deleting the topography did not change the results very much: the standard deviation of the difference between the wind field in the topography-less simulation and in the simulation with the real island was only 0.23. The largest change was found when taking away the heat variation together with surface rough-

ness, or when the entire island was taken away. There was hardly any difference in the standard deviation when deleting the heat variations alone as compared with that when deleting the heat together with topography.

It should be pointed out that the standard deviation of the difference in the wind field between a certain simulation and reference run does not give an exact measure of the importance of a parameter. From a numerical value it is not possible to say if the strength of the wind changed or if the maximum of the wind changed location. However, together with the analysis leading to Fig. 14, it is clear that the temperature variation and surface roughness are very important factors influencing the wind field. The mean of the difference between the wind field in the case with a real island and the other simulations were all close to zero. This is expected because the mean was taken over all the grid points in the

**Table 4.** Results from simulations made to investigate the importance of surface properties. × = the parameter is present in the simulation; – = the parameter is absent. The standard deviation and mean are calculated for the difference between the simulation with a realistic island and the actual simulation.

| Name of simulation                             | Topography | Surface roughness | Heat variations | SD   | Mean   |
|--|------------|-------------------|-----------------|------|--------|
| Realistic island                               | ×          | ×                 | ×               | 0    | 0      |
| No topography                                  | –          | ×                 | ×               | 0.23 | 0.017  |
| No heat difference                             | ×          | ×                 | –               | 1.17 | 0.030  |
| No topography, no heat difference              | –          | ×                 | –               | 1.19 | 0.011  |
| No surface roughness difference                | ×          | –                 | ×               | 0.97 | 0.054  |
| No topography, no surface roughness difference | –          | –                 | ×               | 1.00 | 0.077  |
| No heat, no surface roughness difference       | ×          | –                 | –               | 1.32 | –0.102 |
| No island present                              | –          | –                 | –               | 1.30 | 0.007  |

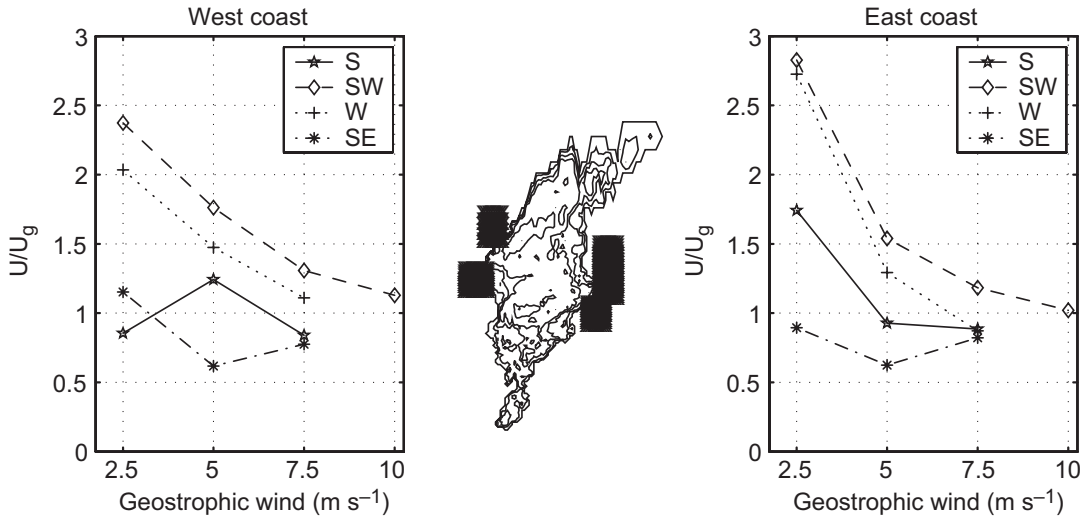


**Fig. 15.** The ratio between modelled mean wind speed and geostrophic wind speed as a function of the geostrophic wind speed. West coast and east coast sites as indicated by the shaded areas on the map are shown respectively. Four different directions of the geostrophic forcing have been used.

domain, and because at some locations the wind was stronger than in the real case while in some other locations it was weaker.

### Supergeostrophic winds at the coasts of Gotland

Simulations with the Baltic computational domain were used to study the occurrence of supergeostrophic winds and their importance for the wind climate.

#### Supergeostrophic winds

The ratio between modelled mean wind speed at the 72 m height at 16:00 LST and geostrophic forcing for four different geostrophic directions and for areas at the west coast and east coast of Gotland are shown in Fig. 15. The shaded areas could be seen as potential wind farms. Results from the model runs covering the whole Baltic Sea area have been used.

The wind generally became more supergeostrophic for low background winds (Fig. 15). The large-scale forcing was then less dominant and the effect of thermally driven flows thus became stronger. The highest winds were found for southwesterly forcing due to the chosen loca-

tions of the sites. If different locations had been chosen, another direction of the forcing would have given the largest ratio (cf. Fig. 10). However, the principles are the same.

For a southwesterly forcing of  $2.5 \text{ m s}^{-1}$ , the modelled wind at the east coast (arithmetic mean of the three shaded areas) was up to 2.8 times higher than the geostrophic wind. The wind climate at the east coast was in this case dominated by a large thermally driven flow (cf. Fig. 3). This resulted in a supergeostrophic jet with a maximum strength at about 100 m height in late afternoon. On the west coast (arithmetic mean of the two shaded areas) the wind also became stronger than the geostrophic wind during the afternoon. The main reason for this was the thermally driven flow originating from the Swedish mainland rather than local effects due to Gotland.

#### Comparison with observations

Measurements showed that the modelled thermally driven winds were indeed also observed. The data from Östergarnsholm and Näsudden were used (Fig. 2). At both sites the measurements were made with cup anemometers mounted on towers, and the data used here were taken at the heights of 28.6 and 75 m. The measured wind speed data were collected from the beginning of

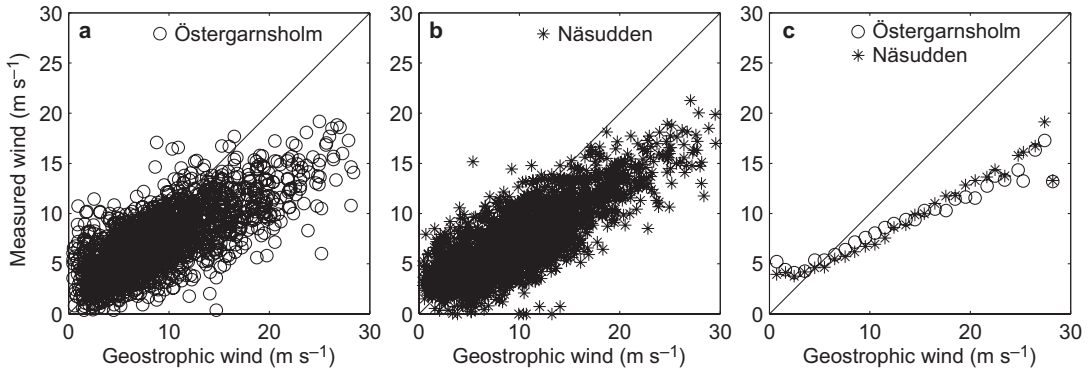


**Fig. 16.** Measured wind speed plotted against the geostrophic wind speed for the years 1995–1998 at two sites: Östergarnsholm (28.6-m height) and Näsudden (75-m height). Plots **a** and **b** show individual measurements, taken at six-hour intervals, while plot **c** shows the average wind speed divided into  $1 \text{ m s}^{-1}$  bins.

June 1995 until the end of December 1998. The geostrophic wind was calculated every 6th hour for the same period, using sea level air pressure fields.

When the observed wind speed for all directions is plotted against the geostrophic wind speed at every sixth hour during the measuring period, it is clear that the measured wind speed decreased compared to the geostrophic wind as the geostrophic wind speed increased (Fig. 16).

When the average of the measured wind speed determined for  $1 \text{ m s}^{-1}$  bins of the geostrophic wind is plotted against the geostrophic wind speed, it is clearly seen that for a geostrophic wind speeds  $< 5 \text{ m s}^{-1}$ , the actual wind speed was generally higher than the geostrophic wind speed due to the mesoscale effects (Fig. 16c). To the contrary, for stronger geostrophic winds ( $> 5 \text{ m s}^{-1}$ ) the actual wind was generally lower than the geostrophic wind speed. This is expected, since in the latter case the friction at the surface became more dominant and the flow could be expected to be more in balance with the large-scale forcing. Since most of the wind data were collected for marine conditions, the waves were also higher at stronger winds, resulting in an increased surface roughness.

## Discussion and conclusions

It has been shown that thermally driven flows affect the wind field (and gradients) not only in coastal areas, but also over large offshore areas

of a semi-enclosed sea like the Baltic Sea. These flows often give rise to sea breezes, low level jets and supergeostrophic winds. For low geostrophic wind speeds ( $< 5 \text{ m s}^{-1}$ ) the diurnal heating of the land areas is the main reason for the modification of the wind climate over the Baltic Sea, whereas for higher wind forcing the changes in the surface roughness between the land and sea also have a large impact. Gotland is too flat in order for the topography to affect the wind field significantly.

Using the advanced mesoscale atmospheric MIUU model it was possible to reproduce the complex features in the wind field that were found in measurements. This made it possible to use the model for studying both spatial and temporal variations in the wind field with a much higher resolution than what would have been possible using observations alone.

Although the wind speed was climatologically higher over sea than over land, it was found that during special conditions the wind speed can also decrease when the air is advected from land out over a cold sea. This phenomenon most likely occurs for strong geostrophic winds when also a strong thermal wind is present. Also the temperature difference between the land and sea has to be large. These factors assist in creating a deeper SBL, which reduces the wind speed at lower heights. If the geostrophic wind is not strong enough, sea breeze circulations start to evolve, giving rise to quite a different situation.

The actual shape of the island and coastline determines the magnitude and horizontal extent

of the flow modifications, when the rest of the forcing (i.e. geostrophic wind, thermal stability, etc.) and surface properties are the same. For all background winds tested, the strongest thermally driven flow appeared behind the right-hand side of the island seen from the direction of the prevailing wind (Fig. 10). A thermal low buildup over the island during the day, being the driving force for the flow modification. To the right this local flow supported the background wind, while to the left it was opposed to it. Over Gotland, the strongest flow was found for southwesterly winds, when the wind entered along the south-eastern coastline of the island.

The size of the thermally driven flow was also dependent on the size of the heated land area. The wind modification originating from the Swedish mainland may affect an area as large as the entire Baltic Sea, illuminating the importance of these flows for the wind climate, as well as of using a large enough model domain. Another important factor is the temperature profile used for the initialisation of the model. With a less stable atmosphere the convective boundary layer may grow higher over an island than for more stable conditions. There are indications that both horizontal temperature gradient and height of the boundary layer are important factors for the magnitude of the thermally driven flow.

The climatological impact of thermally driven flows is not obvious. For different directions of the background flow, the thermally driven wind maxima and minima are located differently. Climatologically some of them will cancel out. They are less pronounced during some parts of the year when the insolation is lower and the sea is relatively warmer compared to land, making the temperature gradient between the land and sea smaller or even reversed. Also, at night the thermally driven flows usually die out. These factors together, shown by Bergström (2001), result in a climatological change in the wind speed that is typically within  $\pm 2\%$  over the Baltic Sea, as compared with a scenario with no temperature changes between the land and sea. However, looking at the root mean square differences for the climatological case, Bergström (2001) showed that the mean change in the wind speed is typically around 10% with extremes of up to 60%. This points to the fact that thermally driven

flows have a large impact on the wind field over the entire Baltic Sea on a shorter time scale. We have shown here that also observations clearly indicate this large impact on annual averages, e.g. resulting in supergeostrophic wind speeds at around 30–75 m height for geostrophic wind speeds below  $5 \text{ m s}^{-1}$ , while the impact decreases with increasing geostrophic wind speed.

It can be concluded that thermally driven flows are climatologically important and affect directly people living in the areas with thermal flow modifications. They are also important for transport of air pollutants and propagation of sound, which may be affected by the sharp gradients of wind (and temperature) that appear in close connection to these flows in coastal areas.

*Acknowledgements:* This work was partly sponsored by the Swedish Energy Agency (STEM), project nr. 11539-2. We would like to thank Professor Ann-Sofi Smedman for good comments on the manuscript and we are grateful to all involved performing the balloon measurements on Gotland in May 2000.

## References

- Alexandersson H. & Bergström H. 1979. *Evaluation of double theodolite pibal tracking data*. Report 56, Department of Meteorology, Uppsala University.
- Andrén A. 1990. Evaluation of a turbulence closure scheme suitable for air-pollution applications. *J. Appl. Meteor.* 29: 224–239.
- Arritt R.W. 1989. Numerical modelling of the offshore extent of sea breezes. *Quart. J. Roy. Meteorol. Soc.* 115: 547–570.
- Arritt R.W. 1993. Effects of the large-scale flow on characteristic features of the sea breeze. *J. Appl. Meteor.* 32: 116–125
- Bergström H. 1996. A climatological study of boundary layer wind speed using a meso- $\gamma$ -scale higher-order closure model. *J. Appl. Meteor.* 35: 1291–1306
- Bergström H. 2001. Boundary-layer modelling for wind climate estimates. *Wind Eng.* 25: 289–299.
- Bergström H., Johansson P. & Smedman A. 1988. A study of wind speed modification and internal boundary-layer heights in a coastal region. *Boundary-Layer Meteor.* 42: 313–335.
- Csanady G.T. 1974. Equilibrium theory of the planetary boundary layer with an inversion lid. *Boundary-Layer Meteor.* 6: 63–79.
- Deardorff J.W. 1978. Efficient prediction of ground surface temperature and moisture, with inclusion of a layer of vegetation. *J. Geophys. Res.* 83: 1889–1903.
- Doran J.C. & Gryning S.E. 1987. Wind and temperature

- structure over a land–water–land area. *J. Clim. Appl. Meteorol.* 26: 973–979.
- Estoque M.A. 1962. The sea breeze as a function of the prevailing synoptic situation. *J. Atmos. Sci.* 19: 244–250.
- Enger L. 1986. A higher order closure model applied to dispersion in a convective PBL. *Atmos. Environ.* 20: 879–894.
- Enger L., Koracin D. & Yang X. 1993. A numerical study of the boundary-layer dynamics in a mount valley. Part 1: Model validation and sensitivity experiments. *Boundary-Layer Meteorol.* 66: 357–394.
- Garrat J.R. 1987. The stably stratified internal boundary layer for steady and diurnally varying offshore flow. *Boundary-Layer Meteorol.* 38: 369–394.
- Garrat J.R. 1990. The internal boundary layer- a review. *Boundary-Layer Meteorol.* 50: 171–203.
- Garrat J.R. & Ryan B.F. 1989. The structure of stably stratified internal boundary layer in offshore flow over the sea. *Boundary-Layer Meteorol.* 47: 17–40.
- Gilliam R.C., Raman S. & Niyogi D.D.S. 2004. Observational and numerical study on the influence of large-scale flow direction and coastline shape on sea-breeze evolution. *Boundary-Layer Meteorol.* 111: 275–300.
- Grisogono B. & Tjernström M. 1996. Thermal mesoscale circulations on the Baltic coast: 2. Perturbation of surface parameters. *J. Geophys. Res.* 101: 18999–19012.
- Gryning S.E. & Joffre S. 1987. Wind structure over the Öresund Strait, paper presented at the Öresund experiment. In: *Proc. Workshop II, Nordic Cooperative Org. for App. Res. Uppsala, Sweden, 13–14 October 1987*, Risø National Laboratory, Roskilde, Denmark, pp. 11–20.
- Gryning S.E., Joffre S. & Doran J.C. 1987. The Öresund Experiment. Wind and temperature structure over land-water-land area. *Boundary-Layer Meteorol.* 41: 309–318.
- Johansson C. & Bergström H. 2005. *A study of the wind field above Gotland*. Wind energy report WE2005:1, Department of Earth Sciences, Uppsala University.
- Koracin D. & Enger L. 1994. A numerical study of the boundary-layer dynamics in a mount valley. Part 2: Observed and simulated characteristics of atmospheric stability and local flows. *Boundary-Layer Meteorol.* 69: 249–283.
- Källstrand B. 1998. Low level jets in a marine boundary layer during spring. *Contr. Atmos. Phys.* 71: 359–373.
- Källstrand B., Bergström H., Højstrup J. & Smedman A. 2000. Mesoscale wind field modifications over the Baltic Sea. *Boundary-Layer Meteorol.* 95: 16–188.
- Melas D. 1989. The temperature structure in a stably stratified internal boundary layer over a cold sea. *Boundary-Layer Meteorol.* 48: 361–375.
- Mellor G. & Yamada T. 1974. A hierarchy of turbulence closure models for planetary boundary layer. *J. Atmos. Sci.* 31: 1791–1806.
- Pielke R.A. 1984. *Mesoscale meteorological modeling*. Academic Press Inc., Orlando.
- Samuelsson P. & Tjernström M. 2001. Mesoscale flow modification induced by land-lake surface temperature and roughness differences. *J. Geophys. Res.* 106: 12419–12435.
- Sandström S. 1997. Simulations of the climatological wind field in the Baltic sea area using a mesoscale higher-order closure model. *J. Appl. Meteorol.* 36: 1541–1552.
- Savijärvi H. 2004. Model predictions of coastal winds in a small scale. *Tellus* 56A: 287–295.
- Savijärvi H., Niemelä S. & Tisler P. 2005. Coastal winds and low-level jets: Simulations for sea gulfs. *Quart. J. Roy. Meteorol. Soc.* 131: 625–637.
- Smedman A., Bergström H. & Grisogono B. 1997. Evolution of stable internal boundary layers over cold sea. *J. Geophys. Res.* 102: 1091–1099.
- Smedman A., Bergström H. & Högström U. 1996. Measured and modelled local wind field over a frozen lake in mountainous area. *Beitr. Phys. Atmosph.* 69: 501–516.
- Stein U. & Alpert P. 1993. Factor separation in numerical simulations. *J. Atmos. Sci.* 50: 2107–2115.
- Stull R.B. 1988. *An introduction to boundary layer meteorology*. Kluwer Academic Publishers.
- Tjernström M. & Grisogono B. 1996. Thermal mesoscale circulations on the Baltic coast: 1. Numerical case study. *J. Geophys. Res.* 101: 18979–18997.